The relationship between vegetation coverage and climate elements in Yellow River Basin, China

Qin Nie, Jianhua Xu

The paper examined the vegetation coverage dynamic and its response to climate elements in Yellow River Basin from 1998 to 2008 by an integrated approach made from series methods including correlation analysis, wavelet analysis, and wavelet regression analysis. The main findings are as follows: (1) Vegetation coverage exhibited significant, positive correlation with temperature and precipitation, but negative correlation with sunshine hours and relative humidity at some sites. The correlation between NDVI and precipitation is closest, followed respectively by temperature, relative humidity, and sunshine hours. Precipitation and temperature are the two major climate elements affecting vegetation coverage dynamics. (2) The vegetation coverage dynamics reflected by NDVI time series presented nonlinear variations that depended on the time-scale. Precipitation and temperature both presented nonlinear variations that were morphologically similar with those of NDVI. These further supported the close relationship between NDVI and these two climate elements from a new perspective. (3) Although NDVI, temperature, and precipitation revealed nonlinear variations at different time scales, the vegetation coverage showed a significantly, positively linear correlation with temperature and precipitation at all the time scales under examination.

PeerJ PrePrints | https://peerj.com/preprints/153v1/ | v1 received: 13 Dec 2013, published: 13 Dec 2013, doi: 10.7287/peerj.preprints.153v1

The relationship between vegetation coverage and climate elements in Yellow River Basin, China

QIN NIE[1, 2], JIANHUA XU[2*]

1. Department of Spatial Information Science and Engineering, Xiamen University of Technology, Xiamen 361024, China. Email: nieqinhongyi@163.com.
2. The Research Center for East-West Cooperation in China, The Key Lab of GIScience of the Education Ministry PRC, East China Normal University, Shanghai 200241, China. Email: jhxu@geo.ecnu.edu.cn.

1. Introduction

Terrestrial ecosystems are permanently changing at a variety of spatial and temporal scales due to natural and/or anthropogenic causes (Martíneza and Gilabert 2009). Climate change is one of the causes resulting in land cover change (Lambin and Strahler 1994). Evidence shows that there is a strong relationship between terrestrial vegetation coverage and climate variability (Kaufmann et al., 2003). Therefore, the study on the relationship between vegetation coverage change and the related climate elements has been more and more attention in the recent years (Fu et al 2007; Yang et al. 2010).

In most existing studies, remote sensing images have typically been used as the test datasets. An example is SPOT VEGETATION product, which can provide the required time-series of satellite images to extract vegetation parameters and monitor dynamic trends in vegetation. Among the surface parameters extracted from remote sensing data, normalized difference vegetation index (NDVI) has proved to be a proxy for the status of the aboveground biomass at the landscape level because of the high correlation with green-leaf density, net primary production and COB_{2B} fluxes (Running and Nemani 1988; Tucker and Sellers 1986; Wylie et al. 2003), which can be calculated by the formula NDVI= (NIR-RED)/(NIR+RED), where NIR and RED are the reflectance in the near-infrared and red electromagnetic spectrums of objects on the earth surface, respectively (Eidenshink and Faundeen, 1994).

Climate elements such as precipitation and temperature, effect the vegetation coverage growth, and NDVI time series have proven useful to reflect the change of vegetation coverage to a certain extent (Nemani et al. 2003). Therefore, the studies on the relationship between NDVI and climate elements have become a hot topic in a much larger context of ecological research (Fu et al. 2007).

Many case studies in different countries and regions have also been conducted to evaluate vegetation dynamic. As a result, several methodologies have been used to monitor vegetation dynamic from multi-temporal data, including statistical methods

* Correspondence to: Jianhua Xu, the Research Center for East-West Cooperation in China, East China Normal University, 200241, Shanghai, China. E-mail: jhxu@geo.ecnu.edu.cn

such as principal component analysis (Hall-Beyer 2003; Hirosawa et al. 1996) and curve fitting (Jonsson and Eklundh, 2004; Zhang *et al.*, 2003), as well as spectral-frequency techniques such as Fourier analysis (Azzali and Menenti 2000; Stockli and Vidale 2004), harmonic analysis (Jakubauskas et al. 2001) and wavelet analysis (Martinez and Gilabert 2009; Galford et al. 2008). However, it has proven difficult to achieve a thorough understanding of the vegetation coverage dynamic mechanism by any individual method (Yang et al. 2012; Liu et al. 2011). Because NDVI and climate elements time series usually present different frequency components, such as seasonal variations, long-term and short-term fluctuations, there is still a lack of effective means available for underlying the vegetation coverage dynamic and its related climate elements at different time scales (Cao et al. 2012; Nie et al. 2012).

The Yellow River Basin (YRB), as one of seven river basins in China, spans across arid, semi-arid, and semi-humid climate zones, which results in rich vegetation types, but with a very fragile ecosystem in part of the basin. Specially, drought and flooding disasters frequently occur in this basin, which is in response to regional climate change (Deng et al. 2007). The basin dominates the ecological stability in north China. It is, therefore, necessary to gain a deep and through understanding of the relationship between vegetation coverage and climate elements in the basin.

In the last 20 years, numerous researches have investigated the relationships between vegetation dynamic and climate elements in YRB (Miao et al. 2012; Liang et al. 2012; Liu et al. 2008), but the majority is of the single-time scale analysis. As mentioned above, the time series of NDVI and climate elements usually characterized by patterns like seasonal variations, long-term trends and localized abrupt changes, thus, a multiple time-scale analysis on these relationships is essential and meaningful. By now, a detailed study of climate-vegetation interaction at multiple time scales, however, has not systematically undertaken in the YRB.

On the other hand, although advances in the relationship between NDVI and climate elements has been taken, the mechanism and extent of the climatic influence on NDVI has not been understood fully, the interaction between temperature, radiation and water imposing complex and varying limitations on vegetation activity. Particularly, few studies could investigate the relationship from morphological similarity. This would support the relationship between NDVI and climate variability from a new perspective.

The objective of the present study is to reveal the relationship between vegetation coverage and major climate elements at multiple time scales in YRB using an integrated approach. Firstly, a correlation analysis was used to identify the major climate elements affecting vegetation coverage based on the data of NDVI time series and the climatic data from 24 meteorological stations. Secondly, a wavelet transform (WT) was used to reveal the nonlinear pattern in changes of vegetation coverage and major climate elements at different time scales, trying to look into the morphological similarity between both temporal patterns. Lastly, the regression analysis was employed to show the quantitative relationship between vegetation coverage and the major climate elements based on results of wavelet analysis at different time scales.

2. Study area and data

2.1 Study area

Originating in the Bayan Har Mountains in Qinghai Province of western China, the Yellow River is the second-longest river in China and the sixth-longest in the world, with the estimated length of 5464km. It flows through nine provinces of China and empties into the Bohai Sea. The Yellow River Basin (Fig.1) ranges between 96 º-119 ºE and 32 º-42 ºN with an area of 794712kmP^{2P}, an east-west extent of 1900km, and a north-south extent of 1100km (Yang et al., 2002). The climate in the basin is continental climate, with humid climate in the south-east, semiarid climate in the middle and arid climate in the north-west. The average annual precipitation is between 200 and 600mm, and drought is the basic characteristic. Together with the complex geomorphic type and the inconsistent topography, the vegetation type is diverse (Fig.1). From east to west, the vegetation consists of warm temperature zone forest, temperate zone forest (meadow) steppe, temperature zone typical steppe, temperate zone desert steppe, temperate zone shrub and semi-shrub desert, alpine shrubs and meadow, and alpine steppe.

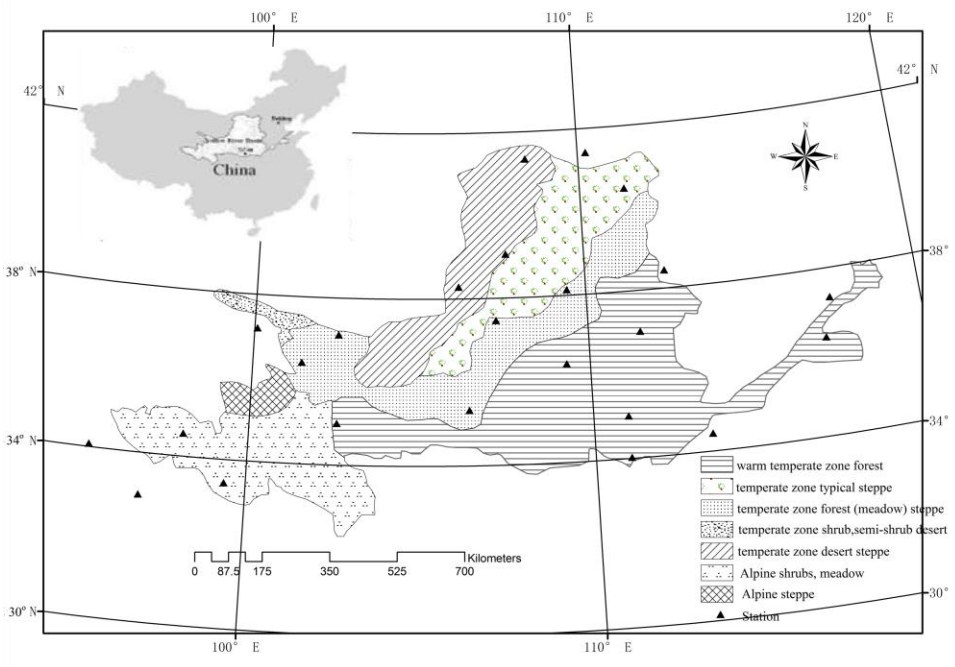

Fig.1 Types of Vegetation Coverage and Selected Metrological Stations in Yellow River Basin

2.2 Climate data

The climate data series from April 1998 to July 2008 were from 24 selected

meteorological stations in YRB (Fig.1), provided by China Meteorological Data Sharing Service System (CMDSSS, http://cdc.cma.gov.cn). The data included ten-day mean temperature (T, 0.1 ℃), ten-day mean precipitation (P, 0.1 mm), ten-day average relative humidity (H, 1 %) and ten-day sunshine hours (S, 0.1 h). The standards of the measurement instruments and data processing have been outlined in the CMDSSS. For these time series, the homogeneity test has been done using SNHT, Buishand and Pettitt homogeneity test method. The 24 stations were fairly evenly distributed in the study region, representing all the vegetation types in YRB, with 4 stations in alpine shrubs, meadow, 9 stations in warm temperate zone forest, 2 stations in temperate zone typical steppe, 1 station in temperate zone shrub, semi-shrub desert, 3 stations in temperate zone desert steppe, and 5 stations in temperate zone forest (meadow) steppe.

2.3 NDVI data

In this research, a time series of 372 SPOT-VGT scenes, covering the period from April 1998 to July 2008, were obtained from the Image Processing and Filing Center of VITO Institute, Belgium, which has been improved by applying atmospheric correction, cloud removal, and bi-directional reflectance distribution function (BRDF) correction (Morawitz et al. 2006). Each 10-day NDVI data was synthesized by a revised Maximum Value Composites (MVC) method. The 10-day periods of synthetic SPOT-VGT scenes were defined as from date 1 to date 10, date 11 to date 20, and date 21 to the end of each month. The spatial resolution was 1 km×1 km, nearly as a constant across the whole 2,250 km swath covered, which meant that there was almost no distortion at the image edge (Maisongrande et al. 2004).

The SPOT-VGT images record the digital number (DN) between 0 and 255. To recalculate digital numbers to proper NDVI values, the grey value of every pixel is linearly stretched by NDVI=DN ×0.004-0.1, which converts the data range to [0, 1]. In order to match the climate data, 24 mete-stations，belonging to different vegetation cover types respectively，were chosen as typical sites to investigate the relationship between NDVI and climate elements. Eight neighboring pixels of each station could cover the station well; therefore, Average NDVI value from eight neighboring pixels was calculated to represent the vegetation cover condition near station. According to Wang et al. (2010), the land use/cover map of YRB in 2000 was obtained (Fig.2), from which, the information on the nature of the land use/cover near stations could be clearly got.

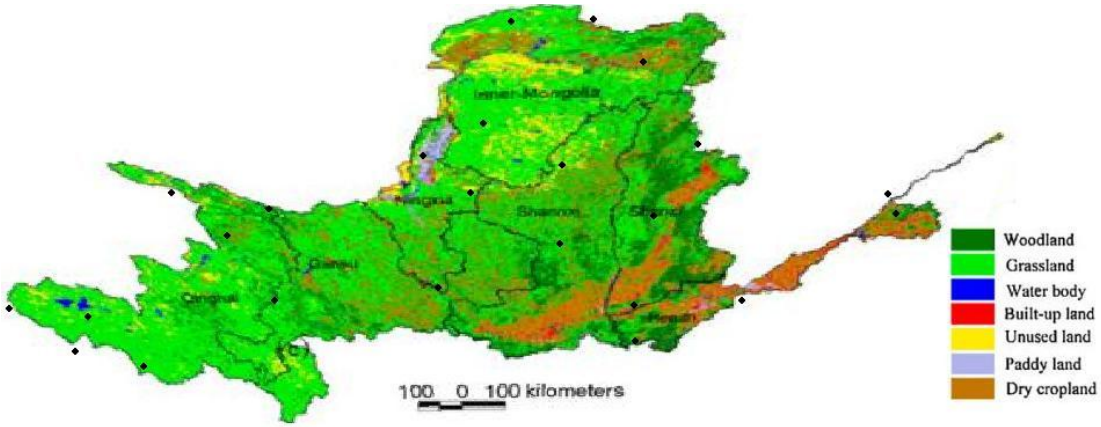

Fig.2 Spatial distribution of Land use in 2000, Yellow River Basin

3 Methodology

Three steps were taken to evaluate different temporal characteristics of NDVI and its relationship with regional climate variables. Firstly, a correlation analysis was employed to identify the major climate elements affecting vegetation coverage. Secondly, WT was used to reveal the periodicity and nonlinear pattern in change of NDVI and major climate elements. Thirdly, a regression analysis was employed to show the quantitative relationship between vegetation coverage and its related climate elements based on the results of WT at different time scales.

3.1 correlation analysis

In this study, Pearson correlation coefficient was used to check the strength of relations between NDVI and the related climate elements (i.e. temperature, precipitation, relative humidity, and sunshine hours), and further identify the major climate elements affecting vegetation coverage change during the period of 1998-2008.

3.2 Wavelet analysis

Wavelet analysis is becoming a common tool for analyzing localized variations of power within a time series. WT uses local basis functions (wavelets) that can be stretched and translated with a flexible resolution in both frequency and time domains to analyze signals. It can be understood as a technique that looks at different sections of the time series with a window adjusted by changing its size, so that a narrow window captures the presence of short-lived events (high frequency variability), whereas a wide window resolves processes that show low frequency variability in time scale (Xu et al. 2009).

The continuous wavelet function that depends on a non-dimensional time parameter η can be written as (Labat 2005):

$$\Psi(\eta) = \Psi(a,b) = |a|^{-1/2}\ \Psi(\frac{t-b}{a}) \tag{2}$$

Where t is time, a is the scale parameter and b is the translation parameter.

For a discrete signal $x(t)$, such as the time series of NDVI, runoff, temperature, or precipitation, its continuous wavelet transform (CWT) can be expressed by the convolution of $x(t)$ with a scaled and translated $\Psi(\eta)$:

$$W_x(a,b) = |a|^{-1/2} \int_{-\infty}^{+\infty} x(t)\Psi^*(\frac{t-b}{a})dt \tag{3}$$

Where $W_x(a,b)$ is the wavelet coefficient, and(*) is the complex conjugate. From this, the concept of frequency is replaced by that of scale. For different combinations of scale a and location b resulting in the decomposition of the signal into time-scale space, a series of wavelet coefficients can be obtained for these specific points. Thus, it can characterize the variation in the signal $x(t)$ at a given time scale.

The wavelet variance $W_x(a)$ can be obtained:

$$W_x(a) = \int_{-\infty}^{+\infty} |W_x(a,b)|^2 db \tag{4}$$

Wavelet variance reflects the energy distribution with scale, and it is usually used to detect the periods present in the signal $x(t)$.

Taking discrete values of a and b, the discrete wavelet transform (DWT) can be defined for signal $x(t)$ (Mallat 1989):

$$x(t) = \sum_k \mu_{j_0,k}\phi_{j_0,k}(t) + \sum_{j=1}^{j_0}\sum_k \omega_{j,k}\psi_{j,k}(t) \tag{5}$$

Where $\varphi_{j0,k}(t)$ and $\Psi_{j,k}(t)$ are the flexing and parallel shift of the basic scaling function, $\varphi(t)$, and the mother wavelet function, $\Psi(t)$, and $\mu_{j0,k}$ $(j<j_0)$ and $\omega_{j,k}$ are the scaling coefficients and the wavelet coefficients, respectively.

A signal can be decomposed according to DWT, allowing separation of the fine-scale behavior from the coarse-scale behavior of the signal (Bruce et al. 2002). Usually, the fine scale corresponds to a compressed wavelet as well as rapidly changing details (high frequency), whereas coarse scale corresponds to a stretched wavelet and slowly changing coarse features (low frequency).

According to the actual criteria for wavelet selection including self-similarity, compactness, and smoothness, symmlet was chosen as the base wavelet. Using this base wavelet, a number of scaling functions were experimented to determine the most suitable wavelet for these datasets of NDVI and climate elements. It was found that 'Sym8' (Fig.2) produced the most robust quantitative results. Therefore, 'Sym8' was chosen as the base wavelet in this paper.

One major interest of this research is to obtain the approximate components based on wavelet decomposition for the time series of NDVI and major climate elements. To accomplish that, the levels analyzed were restricted to S1, S2, S3, S4, and S5 to represent the approximate components. These five time scales are designated as S1

through S5 and started from 20-day (S1), then increased by twofold for the next scale level until a 320-day time scale was attained (S5).

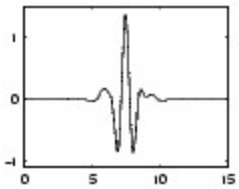

Fig.3 the sym8 wavelet

3.3 Wavelet regression analysis

Wavelet regression analysis (Xu et al. 2008 2011) was conducted to examine the quantitative relationship between NDVI and major climate variables. Firstly, the nonlinear series of NDVI and the relevant climate elements were approximated using wavelet decomposition at multiple time scales; regression analysis method was then used to reveal the statistical relationship between NDVI and the related climate elements based on the results from wavelet approximation.

4 Results

4.1 Major climate elements affecting vegetation coverage

In order to identify the major climate elements affecting vegetation coverage, the NDVI values at the 24 meteorological stations were extracted from the SPOT-VGT Images, and then correlation coefficients was computed based on the times series of 372 data on NDVI, precipitation, temperature, relative humidity, and sunshine hours.

The analytical results (Table 1) indicated that NDVI had a positive correlation with precipitation and temperature, but a negative correlation with relative humidity and sunshine hours at a few sites. The correlation between NDVI and precipitation is closest, followed respectively by temperature, relative humidity, and sunshine hours. Different vegetation types showed little difference in the correlation strengths between NDVI and precipitation and temperature.

Table 1 Correlation coefficients between NDVI and climate elements

No.	Station	NDVI vs P	NDVI vs T	NDVI vs H	NDVI vs S	Vegetation types
1	LuShi	0.820**	0.443**	0.349**	0.106*	warm temperate zone forest
2	HeZuo	0.826**	0.616**	0.613**	0.028	warm temperate zone forest
3	YunCheng	0.775**	0.408**	0.124*	0.514**	warm temperate zone forest
4	Yan'An	0.807**	0.471**	0.356**	0.177**	warm temperate zone forest
5	Ji'Nan	0.807**	0.468**	0.480**	0.156**	warm temperate zone forest
6	JieXiu	0.123*	0.407**	0.444**	0.034	warm temperate zone forest
7	YuanPing	0.841**	0.519**	0.504**	0.265**	warm temperate zone forest
8	ZhengZhou	0.584**	0.182**	0.077	0.396**	warm temperate zone forest
9	HuiMingcounty	0.578**	0.254**	0.246**	0.331**	warm temperate zone forest
10	Hohhot	0.721**	0.515**	0.228**	0.381**	temperate zone typical steppe
11	darfur joint flag Abraham	0.754**	0.480**	-0.048	0.316**	temperate zone typical steppe
12	GangCha	0.787**	0.734**	0.773**	-0.159**	temperate zone shrub,semi-shrub desert
13	PingLiang	0.841**	0.449**	0.362**	0.266**	temperate zone forest (meadow) steppe
14	Xi'Ning	0.809**	0.562**	0.537**	0.196**	temperate zone forest (meadow) steppe
15	YanChi	0.615**	0.307**	0.273**	0.226**	temperate zone forest (meadow) steppe
16	YuLin	0.812**	0.332**	0.118*	0.441**	temperate zone forest (meadow) steppe
17	WuQiaoling	0.806**	0.623**	0.416**	-0.187**	temperate zone forest (meadow) steppe
18	YinChuan	0.839**	0.336**	0.280**	0.466**	temperate zone desert steppe
19	Otog Banner	0.608**	0.407**	0.264**	0.238**	temperate zone desert steppe
20	Urad Middle Banner	0.721**	0.340**	-0.234**	0.505**	temperate zone desert steppe
21	DaRi	0.749**	0.542**	0.571**	0.228**	Alpine shrubs, meadow
22	MaDuo	0.740**	0.529**	0.448**	0	Alpine shrubs, meadow
23	YuShu	0.776**	0.626**	0.630**	0.167**	Alpine shrubs, meadow
24	QuMacai	0.620**	0.435**	0.303**	0.106*	Alpine shrubs, meadow

note: **correlation is significant at the 0.01 level(2-tailed), *correlation is significant at the 0.05 level(2-tailed). P: precipitation T: temperature, H: relative humidity, S: sunshine hours.

The results indicated that the two major climate elements that affect vegetation coverage are precipitation and temperature. So, the following discussion about the climate elements affecting vegetation coverage will focus on precipitation and temperature.

4.2 Nonlinear variations of vegetation coverage depending on the time scale

Based on the SPOT-VGT images, the original NDVI time series for 24 meteorological stations were built. These series all showed a fluctuating characteristic. As shown in the Hohhot station (Fig.4 (a)), the original NDVI time series showed fluctuating patterns of NDVI for the period of 1998-2008. It is difficult to identify any trend of NDVI change. With the ascending time scale from S1 to S5, the approximate components based on DWT were obtained (Fig.4(b,c,d)). According to this, the nonlinear patterns for NDVI changes were analyzed at multiple-time scales.

The wavelet decomposition for the NDVI time series at five time scales resulted in five variants of nonlinear patterns (Fig.4(b,c,d)). The S1 curve (Fig.4(b)) shows 11 peaks with multiple sub-peaks and 10 valleys with sub-valleys, which is smoother

than the original signal but still retains a large amount of residual noise from the raw data. These characteristics indicate that although the NDVI varied greatly throughout the study period, there was a hidden trend. At the 40-day scale, the S2 curve (Fig.4(c)) still retains a considerable amount of residual noise. However, it is much smoother than the S1 curve, which allows the hidden trend to be more apparent. Compared to S2, the S3 curve (Fig.4(d)) retains much less residual noise, and presents obvious periodicity, which is indicated by the 11 peaks without sub-peak and 10 valleys with fewer sub-valleys. Perceptibly, the S4 curve (Fig.4(d)) with no sub-peak and sub-valley is much smoother than the S3 curve, and the trend is more obvious in the S4 curve at the time scale of 160-day. Finally, the S5 curve (Fig.4(d)) at the time scale of 320-day, nearly 1 year, presents a clear pattern. Therefore, the nonlinear patterns of NDVI were found to be dependent on the time scale.

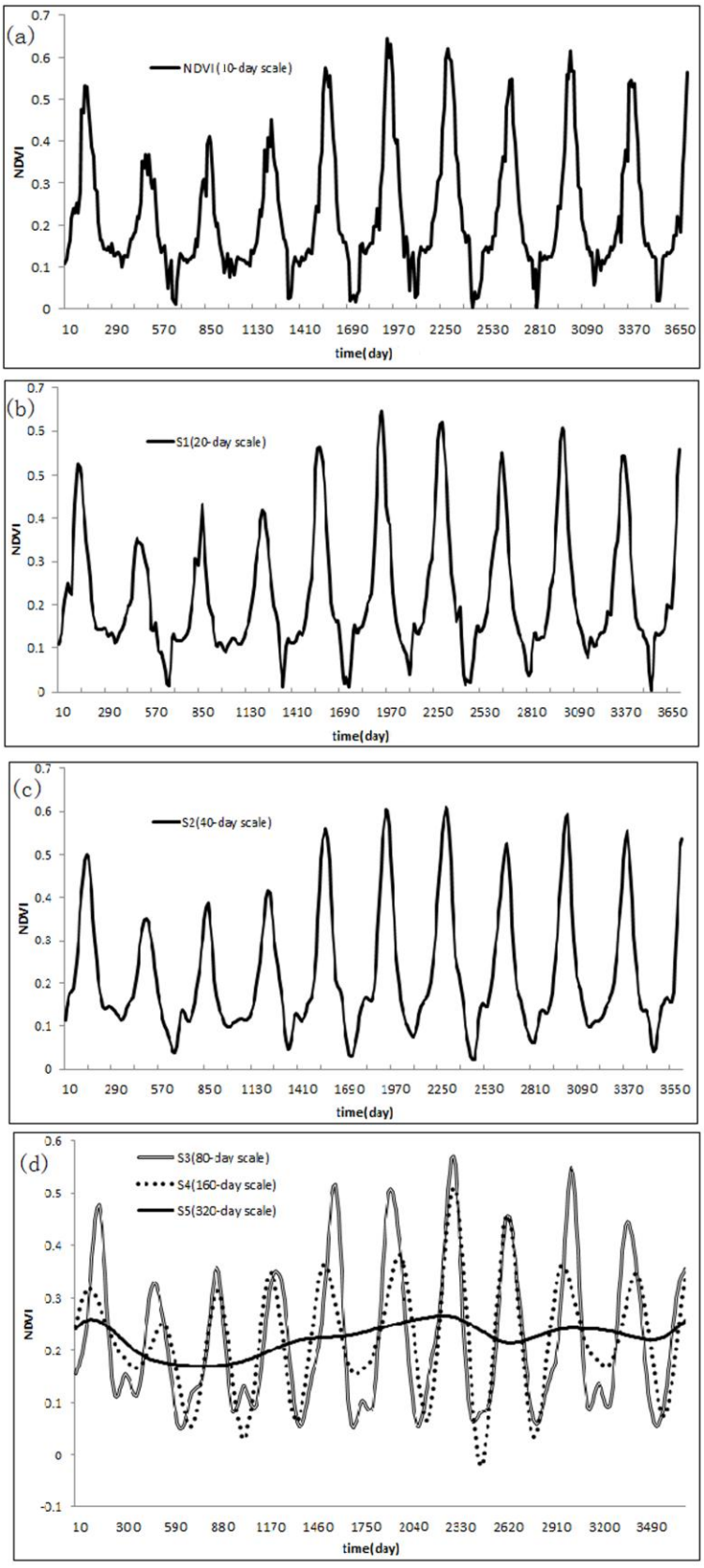

Fig.4 Nonlinear pattern for NDVI at different time scales

4.3 Nonlinear variations of major climate elements depending on the time scale

The approximate components of temperature and precipitation based on DWT were obtained. As illustrated in Fig.5, the five variants of nonlinear patterns from wavelet decomposition on temperature series showed fluctuating patterns of temperature for the period of 1998-2008. The S1 curve shows 11 peaks with multiple sub-peaks and 10 valleys with sub-valleys. Compared to S1, the S2, S3 and S4 curve is incrementally smoother, with less sub-peaks and sub-valleys. Finally, the S5 curve at the time scale of 320-day, nearly 1 year, presents a clear pattern. Therefore, the nonlinear patterns of temperature were found to be dependent on the time scale.

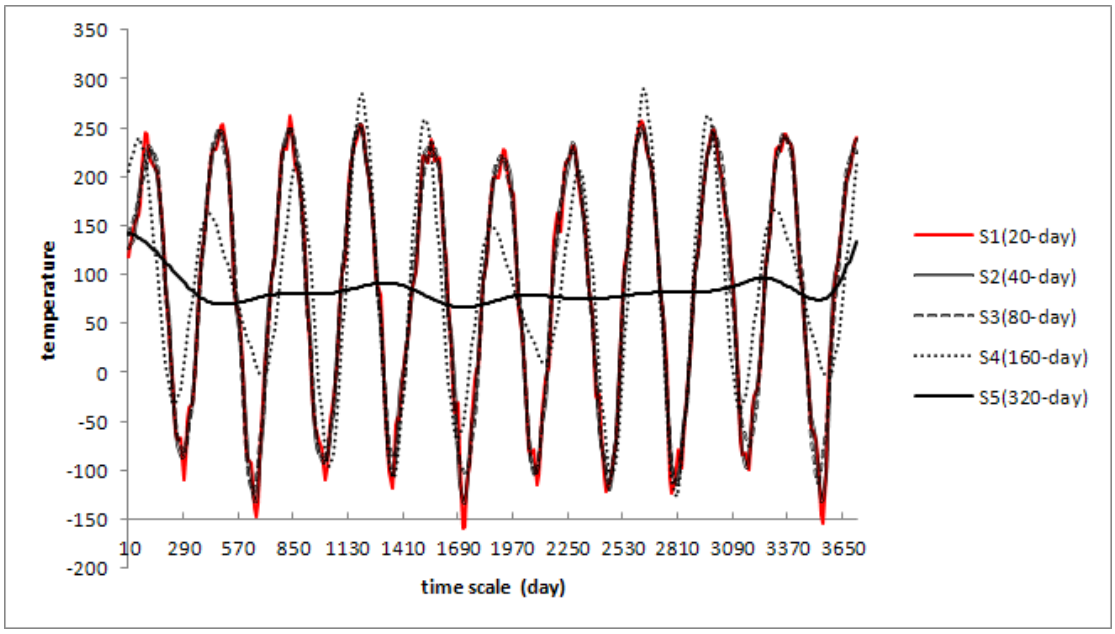

Fig.5 Nonlinear pattern for temperature at different time scales at Hohhot station

Similar observations were also obtained for precipitation (Fig.6). With the ascending time scale from S1 to S4, the curves become increasing smoother, represented by 11 peaks with less sub-peaks and 10 valleys with less sub-valleys, and finally, the S5 curve exhibited an apparent pattern. Hereby, the nonlinear patterns of precipitation were found to be dependent on the time scale.

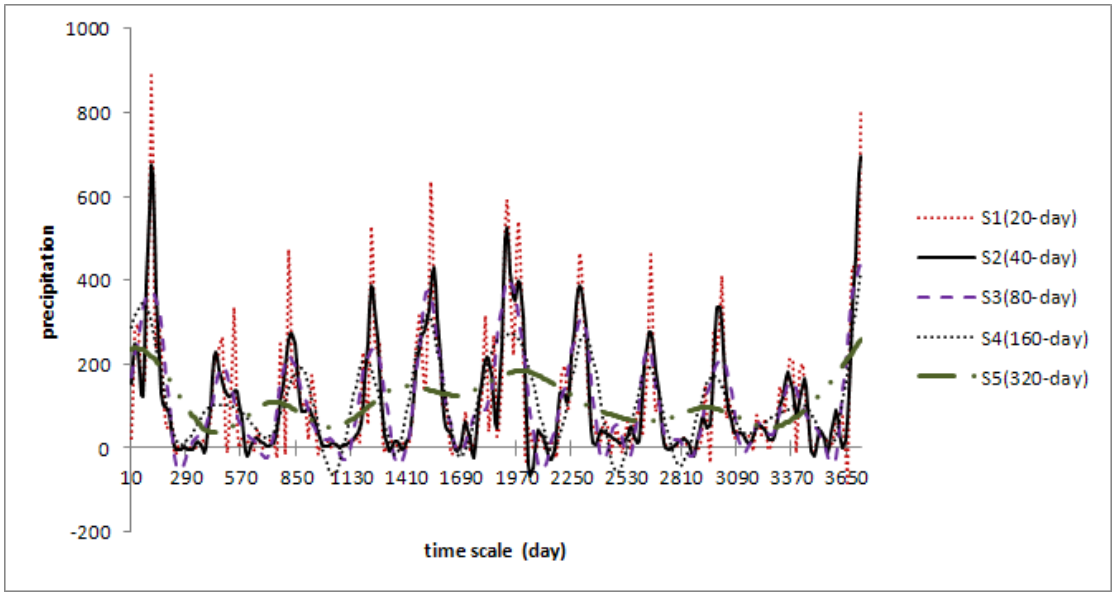

Fig.6 Nonlinear pattern for precipitation at different time scales at Hohhot station

The correlation analysis indicated the existence of climatic impact on the NDVI dynamics in YRB, but it is still instrumental to investigate the morphological similarity between both temporal patterns. From the aforementioned results from wavelet analysis, the nonlinear variations of temperature and precipitation were similar with those of NDVI.

4.4 The relationship between vegetation coverage and climate elements

Based on the close relationship between NDVI and the major climate elements revealed in the above studies, further investigations became necessary to interpret the vegetation dynamic responses to changes in the two major climate variables and establish quantitative relations between them. This was done through the following three steps. Firstly, nonlinear patterns of NDVI, temperature and precipitation were approximated at ascending time scales. Secondly, the statistical relationship between NDVI and the two climate elements were established at given time scales based on the results from wavelet approximation. Finally, the most significant regression models and the most suitable time scales for investigating the NDVI response to the two climate changes were identified.

Table 2 Regression equations between NDVI and climatic elements at different time scales at Hohhot station

Time scale	Regression equation	R2	F	Significance level
S1	N=0.422T+0.507P-0.00412	0.61	289.6	0.005
S2	N=0.371T+0.574P-0.0017	0.65	337.113	0.005
S3	N=0.371T+0.47P-0.028	0.67	381.86	0.005
S4	N=0.38T+0.414P+0.12	0.68	388.49	0.005
S5	N=0.628T+0.08P+0.324	0.27	69.56	0.005

Note: N is 10-day maximum NDVI, p is 10-day average precipitation, T is 10-day average temperature, S1 represents 20-day scale, S2 represents 40-day scale, S3 represents 80-day scale, S4 represents 160-day scale, S5 represents 320-day scale.

The analytical results (Table 2) indicated that each regression model is statistically significant at the 0.005 level. All the regression models yielded meaningful explanations in which NDVI was positively correlated with temperature and precipitation at all the time scales under examination (i.e., 20-day, 40-day, 80-day, 160-day, and 320-day). Furthermore, the regression models at 20-, 40-, 80- and 160-scales have revealed a stronger relationship between NDVI and precipitation, while the regression models at 320-day scale have revealed a stronger relationship between NDVI and temperature. These results provided further evidence supporting the view that the nonlinear pattern of NDVI time series in the study area was influenced by the two climate variables. In addition, the regression model at 160-day scale was the most significant, therefore, the 160-day time scale can be regarded as the most suitable time scale for evaluating the vegetation dynamic responses to climate elements at Hohhot station.

For the other stations, the same steps were done, and the regression models at the most suitable time scales were produced (Table 3). At the stations for forest and alpine shrubs, meadow vegetation, S4 scale (i.e. 160-day) was the most suitable time scale, while at most stations of temperature vegetation, S3 scale (i.e. 80-day) was the most suitable.

The results also suggested that although the time series of NDVI, temperature, and precipitation presented nonlinear patterns, NDVI had a linear correlation with the temperature and precipitation.

Table 3 Regression equations between NDVI and climate elements at the most suitable time scales

Station	Regression equation	RP^{2P}	F	Significance level	Most suitable scale
DaRi	N=0.28P+0.57T+0.1	0.76	575.71	0.005	S4
MaDuo	N=0.42P+0.51T+0.08	0.8	754.95	0.005	S4
YuShu	N=0.53P+0.33T+0.108	0.817	824.9	0.005	S4
QuMacai	N=0.82P+0.131T+0.114	0.726	488.99	0.005	S4
LuShi	N=0.43P+0.57T-0.014	0.95	3584.119	0.005	S4
HeZuo	N=0.44P+0.47T+0.097	0.889	1492.234	0.005	S4
YunCheng	N=0.33P+0.58T+0.094	0.867	1206.5	0.005	S3
Yan'An	N=0.49P+0.37T+0.093	0.816	817.11	0.005	S4
Ji'Nan	N=0.68P+0.35T+0.027	0.892	1526.37	0.005	S4
JieXiu	N=0.77P+0.14T+0.047	0.795	717.55	0.005	S4
YuanPing	N=0.7P+0.25T+0.023	0.928	2380.455	0.005	S4
ZhengZhou	N=0.04P+0.76T+0.17	0.7333	507.34	0.005	S4
HuiMingcounty	N=0.05P+0.74T+0.12	0.752	558.26	0.005	S4
darfur joint flag Abraham	N=0.49P+0.37T+0.07	0.7481	547.845	0.005	S3
GangCha	N=0.92P+0.06T+0.001	0.8422	984.38	0.005	S3
YinChuan	N=0.27P+0.62T-0.06	0.7873	683.2	0.005	S3
Otog Banner	N=0.62P+0.09T+0.097	0.6	277.66	0.005	S3
Urad Middle Banner	N=0.14P+0.47T+0.132	0.6631	363.2	0.005	S3
PingLiang	N=0.35P+0.57T+0.05	0.8848	1416.43	0.005	S4
Xi'Ning	N=0.75P+0.212T+0.019	0.8578	1113.22	0.005	S3
YanChi	N=0.33P+0.27T+0.143	0.5213	200.94	0.005	S3
YuLin	N=0.27P+0.56T+0.08	0.7999	737.52	0.005	S4
WuQiaoling	N=0.62P+0.26T+0.078	0.8855	1427.11	0.005	S4

Note: N is 10-day maximum NDVI, P is 10-day average precipitation, T is 10-day average temperature, S3 represents 80-day scale, S4 represents 160-day scale.

5 Discussions

5.1 NDVI correlation with climate elements

Climate elements affect vegetation growth by changing soil moisture and heat energy. The correlation analysis above indicated that precipitation and temperature are two primary climate parameters that directly impact vegetation growth in a positive fashion in the YRB. Many researches have confirmed the correlations between NDVI and precipitation and temperature in YRB (Hao et. al. 2011; Liang et. al. 2012), but most research is based on monthly or yearly interval and few studies have connected climate elements with 10-day NDVI. In addition, in this study, little difference in correlation strengths between NDVI and precipitation has been found among different vegetation type. However, some studies (Li et. al. 2004) have indicated that the vegetation is more sensitive to precipitation in the middle reaches and upper reaches. The reason is that the spatial-temporal scales employed by different studies are different. Furthermore, the conflicting results indicated that the NDVI response to

climate elements was scale-dependent in the temporal dimension.

It is worth noting that NDVI had a negative correlation with relative humidity at two stations in steppe. The negative statistical correlation is mainly a temperature effect. To detect the correlation between humidity and vegetation cover the use of absolute measures (saturation deficit for example) is necessary. Therefore, further studies and results will be expected.

In addition, this paper investigated the morphological similarity between NDVI and the climatic element temporal patterns, suggesting that the relationship between the NDVI and climate elements could be explored from a new perspective.

5.2 long-term influences of climate elements on NDVI

This study investigated the relationship between vegetation coverage and climate elements only in a study period of 11 years that is not enough compared with the long-term climatic behavior. According to the research of Liu and others (2011), the temperature would apparently increase and precipitation would have a slightly increment in 2050 within the study region, which is the results of global climate change. How would the long-term climatic behavior be influence on NDVI? Therefore, further research would be necessary on a longer investigation period.

6 Conclusions

Using an integrated method including correlation analyses, wavelet analysis and wavelet regression analyses, this study investigated the relationship between vegetation coverage and two main climate elements in YRB by coupling SPOT-VGT image-based NDVI time series (1998-2008) with the climate data from 24 meteorological stations within the study area.

From the previous results, the main findings can be concluded as follows:

(1) There was a close relationship between temporal variations in the NDVI and regional climate elements. NDVI was found to significantly correlate with precipitation and temperature in a positive fashion, but negatively correlate with relative humidity and sunshine hours at a few sites. The correlation between NDVI and precipitation is closest, followed respectively by temperature, relative humidity, and sunshine hours. The high values of correlation coefficients have no doubt revealed that precipitation and temperature were the two major climate elements affecting vegetation coverage.

(2) The nonlinear NDVI pattern was found to be scale-dependent with respect to time. The wavelet decomposition of the NDVI time series at the five time scales resulted in five variants of a nonlinear pattern. With the time scale changing from small to large, the wavelet curves became incrementally smoother and stabilizing onto an obvious tendency.

(3) The approximate components from wavelet decomposition on temperature and precipitation series both showed fluctuating patterns that were scale-dependent in the time domain. With the ascending time scale, the curves become increasing smoother, and finally, an obvious pattern was presented, respectively. These nonlinear variations were found to be similar with those of the NDVI.

(4) At all the time scales (20-, 40-, 80-, 160-, and 320-day) under examination, NDVI and the major climate elements (i.e. temperature and precipitation) were significantly and positively correlated at the 24 stations. The most suitable time scale to investigate the responses of vegetation dynamics to the major climate elements was 80 days for temperature vegetation, as well as 160 days for forest and alpine shrubs, meadow vegetation at most stations.

References

Azzali S, Menenti M. 2000. Mapping vegetation–soil complexes in southern Africa using temporal Fourier analysis of NOAA AVHRR NDVI data. *International Journal of Remote Sensing* 21(5): 973−996.

Bruce LM, Koger CH, Li J. 2002. Dimensionality reduction of hyperspectral data using discrete wavelet transform feature extraction. *IEEE Transactions on Geoscience and Remote Sensing* 40(10): 2331– 2338.

Cao L, Xu JH, Chen YN, Li WH, Yang Y, Hong YL, Li Z. 2012. Understanding the dynamic coupling between vegetation cover and climatic factors in a semiarid region—a case study of Inner Mongolia, China. *Ecohydrology*. DOI: 10.1002/eco.1245.

Deng ZY, zhang Q, Yin XZ, Zhang CJ, Xin JW, Liu DX, Pu JY, Dong AX. 2007. Response of Drought Damage to Arid Climate Change. *JOURNAL OF GLACIOLOGY AND GEOCRYOLOGY* 29(1):114-118.

Eidenshink JC, Faundeen JL. 1994. The 1 km AVHRR global land data set: first stages in implementation. *International Journal of Remote Sensing* 15(17): 3443-3462.

Feng J, Wang T Xie C. 2006. Eco-environmental degradation in the source region of the Yellow River. *Environmental Monitoring and Assessment* 122: 125–143.

Fu XF, Yang ST, Liu CM. 2007. Changes of NDVI and their relations with principal climatic factors in the Yarlungzangbo River Basin. *Geographical Research* 26(1): 60-66.

Fu XF, Yang ST, Liu CM. 2007. Changes of NDVI and their relations with principal climatic factors in the Yarlungzangbo River Basin. *Geographical Research* 26(1): 60-66.

Galford GL, Mustarda JF, Melillob J, Gendrin A, Cerrid CC, Cerrie CEP. 2008. Wavelet analysis of MODIS time series to detect expansion and intensification of row-crop agriculture in Brazil, *Remote Sensing of Environment* 112(2):576-587.

Hall-Beyer M.2003. Comparison of single-year and multiyear NDVI time series principal components in cold temperate biomes, *IEEE Transactions on Geoscience and Remote Sensing* 41: 2568−2574.

Hao FH, Zhang X, Ouyang W, Skidmore AK, Toxopeus AG. 2011. Vegetation NDVI Linked to Temperature and Precipitation in the Upper Catchments of Yellow River. *Environ Model Assess* DOI 10.1007/s10666-011-9297-8.

Hirosawa Y, Marsh SE, Kliman DH. 1996. Application of standardized principle component analysis to land-cover characterization using multitemporal AVHRR data. *Remote Sensing of Environment* 58(3): 267-281.

Jakubauskas ME, Legates DR, Kastens JH. 2001. Harmonic analysis of time-series AVHRR NDVI data. *Photogrammetric Engineering and Remote Sensing* 67(4) : 461-470.

Jonsson P, Eklundh L. 2004. TIMESAT— a program for analyzing time-series of satellite sensor data. *Computers & Geosciences* 30(8): 833−845.

Kaufmann RK, Zhou L, Myneni RB, Tucker CJ, Slayback D, Shabanov NV, Pinzon J. 2003. The effect of vegetation on surface temperature: a statistical analysis of NDVI and climate data. *Geophysical Research Letters* 30(22): 2147.

Lambin E, Strahler A. 1994. Indicators of land-cover change for change-vector analysis in multi-temporal space at coarse spatial scales. *International Journal of Remote Sensing* 15(10): 2099-2119.

Li CH,Yang ZF. 2004. Spatio-temporal changes of NDVI and their relations with precipitation and runoff in the Yellow River Basin. *GEOGRAPHICAL RESEARCH* 23(6): 753-759.

Liang SH, Ge SM, Wan L, Xu DW. 2012. Characteristics and causes of vegetation variation in the source regions of the Yellow River, China. *International Journal of Remote Sensing* 33(5): 1529-1542.

Lindsay RW, Percival DB, Rothrock DA. 1996. The discrete wavelet transform and the scale analysis of the surface properties of sea ice. *IEEE Transactions on Geoscience and Remote Sensing* 34: 771−787.

Liu JG, Diamond J. 2008. Revolutionizing China's environmental protection. *Science* 319 (4):37–38.

Liu JG, Li SX, Ouyang ZY, Tam C, Chen XD. 2008. Ecological and socioeconomic effects of China's policies for ecosystem services. *Proceedings of National Academy of Sciences* 105 (28): 9477–9482.

Liu Q, Yang ZF, Cui BS. 2008. Spatial and temporal variability of annual precipitation during 1961–2006 in Yellow River Basin, China. *Journal of Hydrology* 361: 330– 338.

Liu WB, Cai TJ, Ju CY, Fu GB, Yao YF, Cui XQ. 2011. Assessing vegetation dynamics and their relationships with climatic variability in Heilongjiang province, northeast China. *Environmental Earth Sciences* 64(8): 2013-2024.

Liu JF, Wang JH, Jiao MH, Zhang RG. 2011. Response of Water Resources in the Yellow River Basin to Global Climate Change. *Journal of Arid Land* 28(5):860-865.

Mallat SG. 1989. A theory for multiresolution signal decomposition: the wavelet representation. *IEEE Transactions on Pattern Analysis and Machine Intelligence* 11(7): 674–693.

Maisongrande P, Duchemin B, Dedieu G. 2004. VEGETATION/SPOT: an operational mission for the Earth monitoring; presentation of new standard products. *International Journal of Remote Sensing* 25(1): 9–14.

Martinez B, Gilabert MA. 2009. Vegetation dynamics from NDVI time series analysis using the wavelet transform. *Remote Sensing of Environment* 113(9):1823-1842.

Miao CY, Yang L, Chen XH, Gao Y. 2012. The vegetation cover dynamics (1982–2006) in different erosion regions of the Yellow River Basin, China. *Land Degradation & Development* 23(1):62-71.

Morawitz D. 2006. Using NDVI to assess vegetative land cover change in central Puget Sound. *Environmental Monitoring and Assessment* 114(1): 85-106.

Nemani RR, Keeling CD, Hashimoto H, Jolly WM, Piper SC, Tucker CJ, Myneni RB, Running SW. 2003. Climate-driven increases in global terrestrial net primary production from 1982 to 1999. *Science* 300(5625):1560–1563.

Nie Q, Xu JH, Ji MH, Cao L, Yang Y, Hong YL. 2012. The vegetation coverage dynamic coupling with climatic factors in Northeast China Transect. *Environmental Management* 50(3): 405-417.

Running SW, Nemani R. 1988. Relating seasonal patterns of the AVHRR vegetation index to simulated photosynthesis and transpiration of forests in different climates. *Remote Sensing of Environment* 24: 347-367.

Stockli R, Vidale PL. 2004. European plant phenology and climate as seen in a 20-year AVHRR land-surface parameter dataset. *International Journal of Remote Sensing* 25(17): 3303−3330.

Tucker CJ, Sellers PJ. 1986. Satellite remote sensing of primary production. *International Journal of Remote Sensing* 7: 1395-1416.

Xu JH, Chen YN, Ji MH, Lu F. 2008. Climate change and its effects on runoff of Kaidu River, Xinjiang, China: A multiple time-scale analysis. *Chinese Geographical Science* 18(4): 331-339.

Xu JH, Chen YN, Li WH, Ji MH, Dong S, Hong YL. 2009. Wavelet Analysis and Nonparametric Test for Climate Change in Tarim River Basin of Xinjiang during 1959-2006. *Chinese Geographical Science* 19(4): 306-313.

Xu JH, Li WH, Ji MH, Lu F, Dong S. 2010. A comprehensive approach to characterization of the nonlinearity of runoff in the headwaters of the Tarim River, Western China. *Hydrological Processes* 24(2): 136-146.

Xu JH, Chen YN, Lu F, Li WH, Zhang LJ, Yang Y. 2011. The nonlinear trend of runoff and its response to climate change in the Aksu River, western China, *International Journal of Climatology* 31(5): 687-695.

Yang Y, Xu JH, Hong YL, Lv GH. 2012. The dynamic of vegetation coverage and its response to climate elements in Inner Mongolia, China. *Stochastic Environmental Research and Risk Assessment* 26(3): 357-373.

Yang ZF, Li CH, Huang GH, Cai YP. 2010. Analysis of relationships between NDVI and climatic/hydrological parameters in the Yellow River basin. *International Journal of Environment and Pollution* 42: 166-183.

Yang ST, Liu CM, Sun R. 2002. The Vegetation Coverage over Last 20 Years in

Yellow River Basin. *ACTA GEOGRAPHICA SINICA* 57(6): 679-684.

Wang G, Innes JL, Lei J, Dai S, Wu SW. 2007. China's forestry reforms. *Science* 318: 1556–1557.

Wang SY, Liu JS, Ma TB. 2010 Dynamics and changes in spatial patterns of land use in Yellow River Basin, China. *Land Use Policy* 27 :313–323.

Wylie BK, Johnson DA, Laca E, Saliendra NZ, Gilmanov TG, Reed BC. 2003. Calibration of remotely sensed, coarse resolution NDVI to CO2 fluxes in a sagebrush steppe ecosystem. *Remote Sensing of Environment* 85: 243-255.

Zhang X, Friedl MA, Schaaf CB, Strahler AH, Hodges JCF, Gao F. 2003. Monitoring vegetation phenology using MODIS. *Remote Sensing of Environment* 84: 471−475.

Zhou HK, Zhao X, Tang Y, Gu,S, Zhou L. 2005. Alpine grassland degradation and its control in the source region of the Yangtze and Yellow Rivers, China. *Grassland Science* 51:191–203.

Zhou HJ, Rompaey AV, Wang JA. 2009. Detecting the impact of the "Grain for Green" program on the mean annual vegetation cover in the Shaanxi province, China using SPOT-VGT NDVI data. *Land Use Policy* 26:954–960.

Zhou DC, Zhao SQ, Zhu C. 2012. The Grain for Green Project induced land cover change in the Loess Plateau: A case study with Ansai County, Shanxi Province, China. *Ecological Indicators* 2012:88-94.